3. Results

3.1 ECP and Potentiodynamic Measurements

3.1.1 Low–Temperature Tests at Ambient Pressure

The ECP of A533 Gr.–B, Alloy 600, and 308 SS clad were measured in saturated boric acid solution at ≈95°C and ambient pressure. Typical plots of ECP vs. time for the three materials are shown in Fig. 27. The results show a large increase in the ECP of 308 SS clad and a slight increase for Alloy 600 within the few hours of exposure; the ECP of A533 Gr.–B steel is lower than the other alloys and did not change with time. The increase in ECP of 308 SS clad and Alloy 600 is due to the formation of a protective oxide layer, whereas the surface of A533 Gr.–B steel stays bare, indicating dissolution or corrosion. The ECPs of A533 Gr.–B steel, Alloy 600, and 308 SS clad in boric acid solutions with different B content at 95°C and ambient pressure are compiled in Table 3.

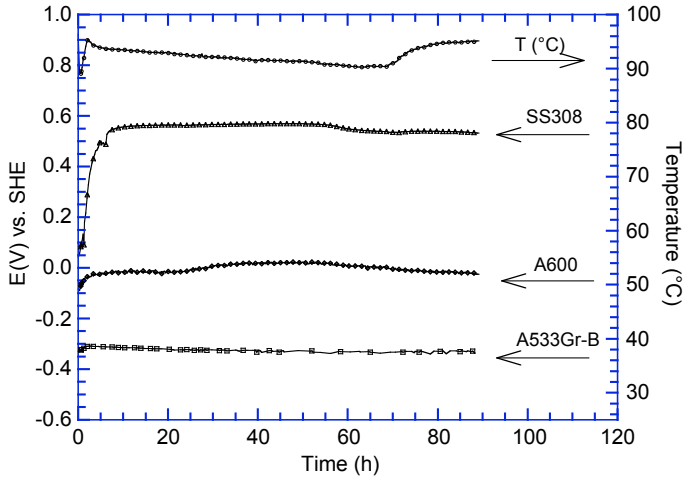

Figure 27.
Typical plot of measured ECP vs. time for the A533 Gr.-B, Alloy 600, and 308 SS in saturated boric acid solution at ≈95°C and ambient pressure.

Table 3. The ECP of A533 Gr.–B, Type 304 SS, 308 SS weld metal, and Alloy 600 in boric acid solutions at 95°C and ambient pressure.

B Content (wppm)	Gas Environment	ECP (V vs. SHE)			
		A533 Gr.–B	308 SS Weld	304 SS	Alloy 600
36,00	Aerated	-0.332	0.478	0.314	0.151
	Deaerated	-0.296	–		
9,09	Aerated	-0.295	–		
3,56	Aerated	-0.433	–		
	Deaerated	-0.450	–		

Several potentiodynamic tests were also performed on A533 Gr.–B low–alloy steel, Alloy 600, and Type 304 SS in aerated and deaerated solutions of boric acid containing 3500 or 36,000 wppm B at ≈95°C. Figure 28 shows the current density vs. applied potential (vs. SHE) plots for Type 304 SS in aerated saturated solution of boric acid containing 36,000 ppm B at 95°C. The results show a plateau, indicating passivation. For austenitic SSs and Alloy 600, because of changes in the surface condition, the corrosion potential typically shifts to a higher value after passivation.

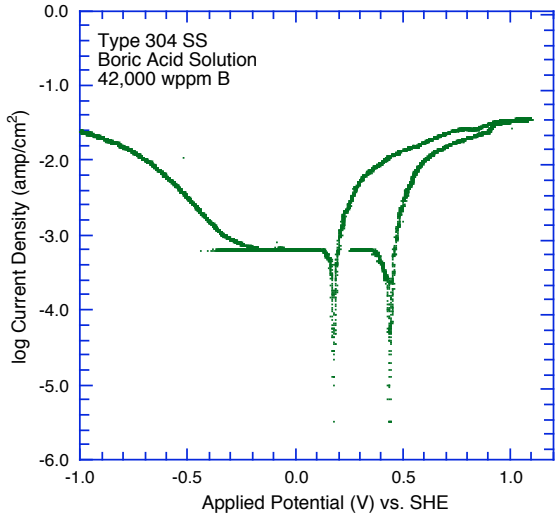

Figure 28.
Potentiodynamic test results for Type 304 stainless steel in aerated saturated solution of boric acid (36,000 wppm B) at ≈100°C.

Figure 29 shows the potentiodynamic test result for the A533 Gr.–B low–alloy steel in the aerated saturated boric acid solution at ≈95°C. The A533 Gr.–B low–alloy steel did not show any passivation behavior. Even after several potential scan cycles, corrosion potential remained the same. Corrosion rates were estimated from the current density vs. potential plots using Faraday's law and the $Fe \rightarrow Fe^{+2} + 2e^{-}$ reaction. The corrosion current density obtained from the potentiodynamic test, i.e., J_{corr} = 4 mA/cm^2 at E_{corr} = -0.342 V (SHE), agrees well with the corrosion rates obtained from corrosion/wastage tests discussed in the next section. The significant results from these tests are summarized below.

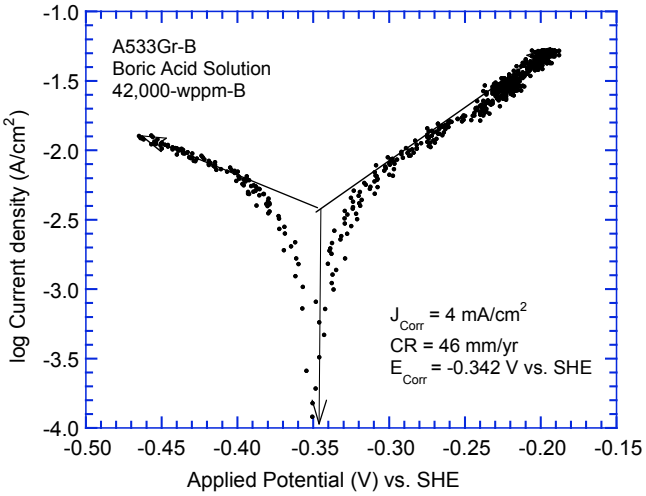

Figure 29.
Potentiodynamic test results for A533 Gr.–B steel in an aerated saturated boric acid solution at 95°C.

For tests in boric acid solution with 36,000 wppm B, the aerated solution turned reddish brown after the test and contained dark brown particles, whereas the deaerated solution remained colorless and contained dark magnetic particles. The solubility of boric acid in water at ≈95°C is slightly greater in deaerated than aerated solutions. Estimated corrosion rates were a factor of ≈3 higher in aerated solution than deaerated solution.

For tests in boric acid solution with 3500 wppm B, both aerated and deaerated solutions remained colorless and contained dark magnetic particles that were identified by x–ray

diffraction analyses as a mixture of maghemite (γ–Fe_2O_3) and magnetite (Fe_3O_4). The A533 Gr.–B low–alloy steel developed a very rough, black, and porous surface layer, whereas a thin, loosely–adherent white film was formed on Type 304 SS and Alloy 600. X-ray diffraction analyses indicated mixtures of boric acid, Fe_2O_3 iron oxide (maghemite–C or γ Fe_2O_3 and hematite), and iron borate FeB_2O_4, on the surface of A533–Gr. B steel. Nickel oxide (NiO), nickel chromium oxide ($NiCr_2O_4$), and nickel–oxide–hydroxide were identified on the Alloy 600 specimen. The A533–Gr. B steel exhibits a heavily reacted porous surface, shown in Fig. 30. Estimated corrosion rates were a factor of ≈1.5 higher in aerated solution than in deaerated solution.

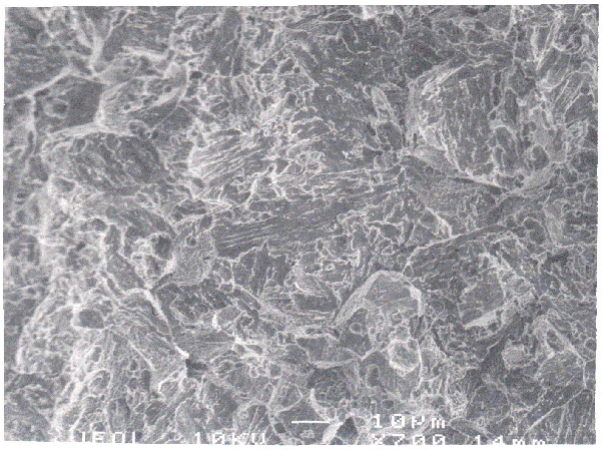

Figure 30.
Photomicrograph of A533 Gr.–B low–alloy steel tested in deaerated boric acid solution containing 3500 wppm B at 95°C.

3.1.2 Tests in Molten H–B–O System at Ambient Pressure

Figure 31 shows the result of a potentiodynamic test on A533 Gr.–B steel in the H–B–O system at 290°C. The H-B-O melt was equilibrated at 290°C for ≈12 h in air. The measured current density throughout the test indicates a very protective surface layer; the results indicate that in the absence of moisture, A533 Gr.–B steel would show negligible corrosion in molten HBO_2.

Figure 32 shows the scenario that occurs during a potentiodynamic test conducted in the H–B–O system with addition of water. It gives a representation of current density as a function

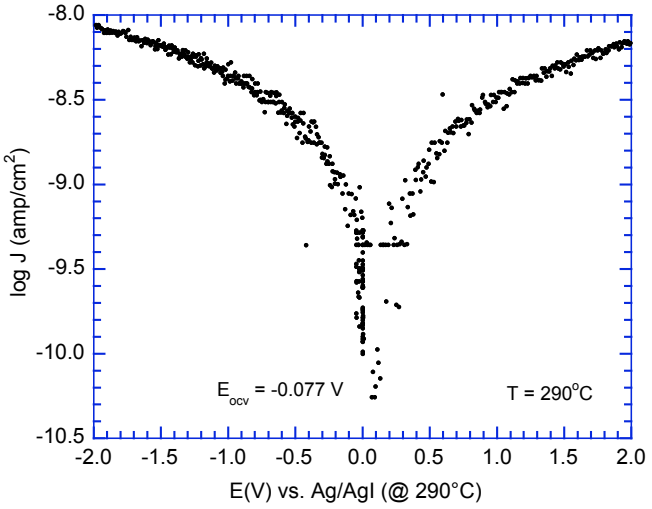

Figure 31.
Potentiodynamic test on A533 Gr.–B steel in molten H-B-O system at 290°C.

of sweeping voltage between +2 to –2. The experiment was started at 290°C with water injection, and the current density increased significantly when the water was introduced into the chamber (depicted by Regions "1" and "2" in Fig. 32). At +2 V, the sweeping direction was reversed till the voltage reached –2 V (Regions 3 and 4), at which point the volatgae direction was reversed again and continued sweeping (Regions 5 through 8). As the moisture evaporates, the current density decreased to a low value similar to that observed in a dry system. (Note that the temperature in the system during the experiment could not be maintained constant due to the addition and evaporation of moisture.) The experiment does show that a significant increase in current density can be attained by the deliberate addition of water to the H-B-O system at elevated temperatures.

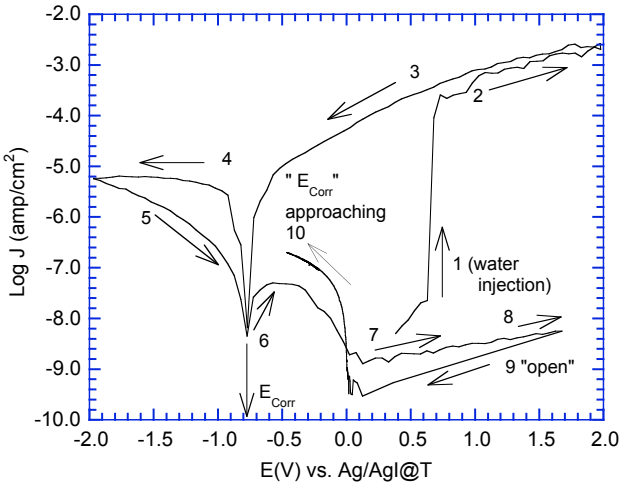

Figure 32.
Potentiodynamic test on A533 Gr.–B steel in molten HBO_2 + B_2O_3 system with addition of water.

3.1.3 Tests in High–Temperature High–Pressure Aqueous Solutions

The ECP of A533 Gr.–B steel, Alloy 600, 308 SS clad, and Pt wire in PWR water with 1000 or 9090 ppm B, ≈2 ppm Li, <10 ppb DO, and ≈2 ppm dissolved hydrogen at 25–316°C and 12.4 MPa (1800 psi) pressure are compiled in Tables 4 and 5. The change in ECP with temperature for the two water chemistries is plotted in Figs. 33a and b. In general, the ECP of all alloys decreased with an increase in temperature. At temperatures below 150°C, the ECP of A533 Gr.–B low–alloy steel is significantly lower than that of the other alloys, and at higher temperatures, the ECPs of all alloys in the two environments are comparable.

Table 4. Measured ECP (mV vs. SHE) of various alloys in water containing 9,090 ppm B, 2 ppm Li, and ≈2 ppm dissolved hydrogen at temperatures between 25 and 316°C and 12.4 MPa pressure

Temperature (°C)	A533 Gr.–B	Alloy 600	308 SS Clad	Pt
25	-0.455	0.026	0.176	0.176
100	-0.487	-0.098	-0.011	-0.040
130	-0.491	-0.152	-0.176	-0.166
150	-0.500	-0.400	-0.196	-0.210
200	-0.543	-0.487	-0.298	-0.469
288	-0.577	-0.598	-0.505	-0.606

Table 5. Measured ECP (mV vs. SHE) of various alloys in water containing 1,000 ppm B, 2 ppm Li, and ≈2 ppm dissolved hydrogen at temperatures between 150 and 316°C and 12.4 MPa pressure

Temperature (°C)	A533 Gr.–B	Alloy 600	308 SS Clad	Pt
150	-0.459	-0.504	-0.420	-0.420
200	-0.565	-0.568	-0.545	-0.567
250	-0.640	-0.638	-0.636	-0.637
288	-0.701	-0.696	-0.697	-0.693
316	-0.746	-0.740	-0.743	-0.739

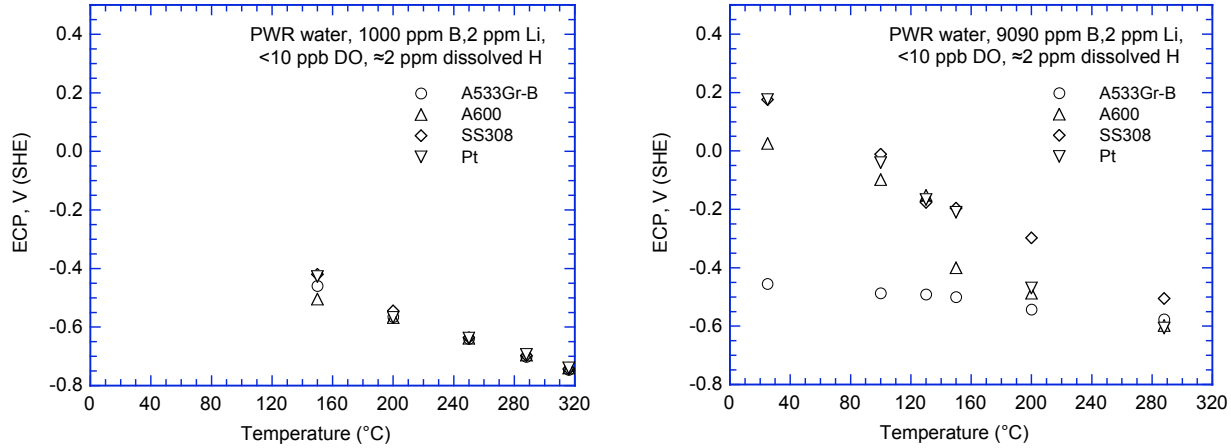

Figure 33. Change in ECP of A533 Gr.–B steel, Alloy 600, and 308 SS weld metal in water containing 1,000 or 9,090 ppm B, 2 ppm Li, and ≈ 2 ppm dissolved hydrogen at temperatures between 150 and 316°C and 12.4 MPa pressure.

3.2 Wastage Corrosion Tests

Corrosion tests were performed to measure the wastage rates of A533B pressure vessel steel, Alloy 600, and Type 308 SS cladding in the boric acid solutions of varying concentrations at 100–316°C under aerated and deaerated conditions. Corrosion tests at 97.5°C and ambient pressure were performed in saturated (37000 wppm B) and half-saturated (18500 wppm B) solutions of boric acid, simulated PWR water (1000 wppm B), and ultra high purity (UHP) water. In addition, tests were conducted in molten boric acid and boric oxide mixtures under pressure and humidity condition that provide chemical compound stability for the molten species. The corrosion tests in the temperature range between 150 and 170°C in the ambient atmosphere were conducted with and without adding water to the boric acid. Corrosion tests at 100-316°C (212–600°F) and 12.4 MPa (1800 psi) were performed in flowing room–temperature saturated boric acid solution under a hydrogen cover gas.

3.2.1 Saturated Boric Acid Solution at 97.5°C

Corrosion tests were conducted on ring specimens of A533 Gr.–B low alloy steel, Alloy 600, and Type 308 SS weld cladding, at 97.5°C in aerated solutions of boric acid that were saturated (37,000 wppm B) or half–saturated (18,500 wppm B) at the test temperature. Tests were also conducted in deaerated saturated solutions of boric acid at 97.5°C. Insulating O–rings were placed at several locations in the stack to protect against galvanic effects between

adjacent samples and/or to serve as spacers. Rubber spacers were also placed at both ends of the stack to provide protection from edge corrosion. The specimens were rotated at 50 rpm to simulate flow. Corrosion rates were determined from measurements of specimen wall thickness for time periods between 24 and 411 h. The average corrosion rates are given in Table 6 for A533 Gr.–B low-alloy steel in aerated and deaerated saturated boric acid solutions, and in Table 7 for aerated half–saturated solution of boric acid.

A significant difference in the corrosion behavior was observed between the Alloy 600 and 308 SS cladding and A533 Gr.–B specimens. The corrosion rates for Alloy 600 and Type 308 SS cladding were found to be negligible compared to those for A533 Gr.–B steel. Figure 34 shows photographs of the specimen holder immediately after 100–h exposure to aerated saturated boric acid solution at 97.5°C and after the specimens were rinsed in ultra-high-purity water. A photograph of the ring test specimens and the specimen holder after 411–h exposure to aerated saturated solution of boric acid is shown in Fig. 35, and individual specimens exposed to various specimens are shown in Fig. 36. After exposure, the A533 Gr.–B samples were covered with dark deposits, Fig. 34(a), but after rinsing they had a shiny metallic surface, Fig. 34(b). In contrast, the Type 308 clad specimens had a shiny surface and showed no corrosion.

Table. 6. Average corrosion rates for A533 Gr.–B low-alloy steel in aerated and deaerated saturated solutions* of boric acid at 97.5°C.

Corrosion Rate Measurement Times		Ave. Corrosion Rate for the Time Interval (mm/y)		
Time Interval (h)	Specimen Exposure Time (h)	Aerated Solution	Deaerated Solution	Remarks
0 – 24	24	93.1	125.2	Samples stacks were rotated at 50 rpm. Aerated condition: open to the air. Deaerated condition: purged with 1%H_2-N_2 gas.
0 – 76	76	60.5	53.4	
24 – 100	76	58.8	71.2	
0 – 100	100	67.0	84.2	
0 – 311	311	42.7	25.1	
100 – 411	311	42.3	26.4	
0 – 411	411	48.3	40.5	

*The same solutions were maintained for 411 h.

Table 7. Average corrosion rates for A533 Gr.–B low-alloy steel in aerated saturated and half-saturated solutions* of boric acid at 97.5°C.

Corrosion Rate Measurement Times		Corrosion Rate at 97.5°C (mm/yr)		
Time Interval (h)	Specimen Exposure Time (h)	Saturated BA Solution (37,000 wt. ppm B)	Half-Saturated Boric Acid Solution (18,500 wt. ppm B)	Ratio of Corrosion Rate in Saturated Solution to that in Half-Saturated Solution
0 – 24	24	93.1	40.7	2.294
0 – 76	76	60.5	24.7	2.452
24 – 100	76	58.8	28.6	2.054
0 – 100	100	67.0	31.5	2.127
0 – 311	311	42.7	16.7	2.564
100 – 411	311	42.3	20.6	2.053
0 – 411	411	48.3	23.3	2.073

*The same solutions were maintained for 411 h.

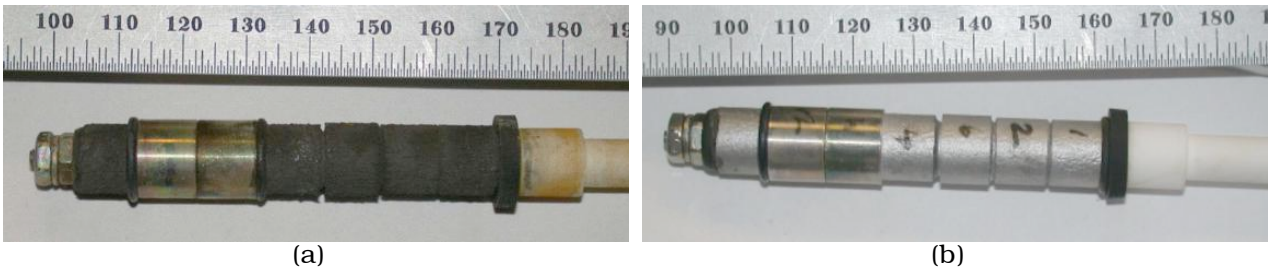

(a) (b)

Figure 34. Ring-test specimen holder (a) after 100-h exposure in aerated saturated boric acid solution at 97.5°C and (b) after rinsing in ultra high–purity water.

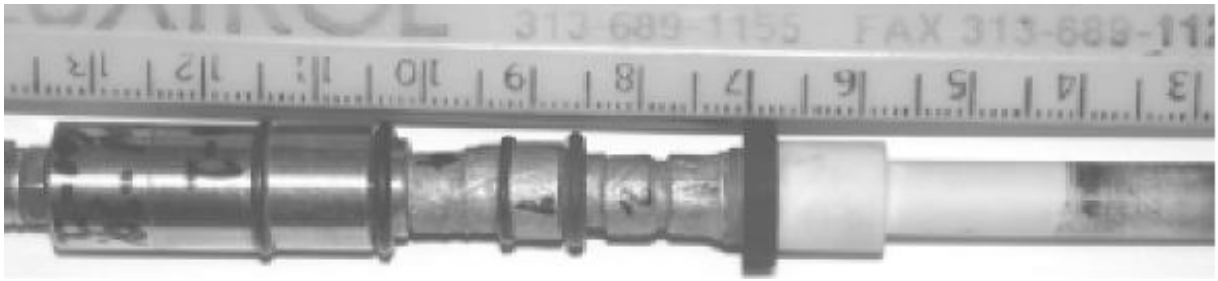

Figure 35. Ring-test specimen holder after 411–h exposure to aerated saturated boric acid solution at 97.5°C.

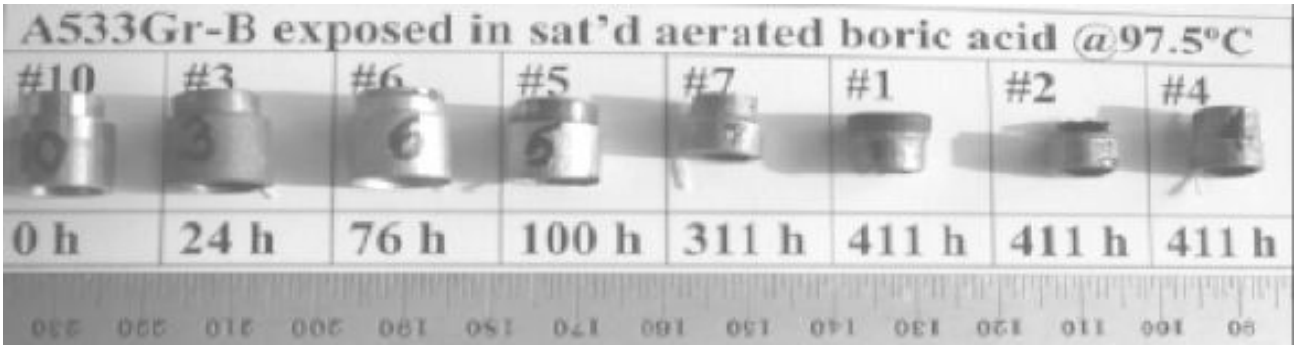

Figure 36. A533 Gr.–B specimens exposed to aerated saturated boric acid solution at 97.5°C for times up to 411 h.

The average corrosion rates of A533 Gr.–B steel in various boric acid solutions at 97.5°C are shown in Fig. 37. The rates determined from short exposure periods, e.g., 24 h, are generally higher than those determined from longer exposure periods. The corrosion rates in half–saturated solution are a factor of ≈2 lower than in saturated solution; the rates for deaerated solution are slightly lower than in aerated solution. The higher rates for short–term tests most likely are due to higher reactivity of a fresh solution. The corrosion rate from a 24–h test in deaerated half–saturated solution of boric acid that was earlier used for a 411–h corrosion test (closed symbols in Fig. 37) is comparable to the rates observed for the long–term tests.

Figure 38a shows the A533-Gr B low-alloy steel ring specimen exposed to saturated boric acid solution at 97.5°C for 311 h; the cross sectional view of the original specimen is shown in Fig. 38b. The top and bottom portions of the specimen have corroded away. Also, the overall surface morphology is similar to that observed in the large cavity observed near the Davis Besse nozzle #3. Figure 38c shows the SEM micrograph of the surface near the edge of the specimen. Figure 38d shows an SEM micrograph of the cross section of the edge of the specimen exposed for 311 h in a saturated boric acid solution at 97.5°C. A very porous part of the sample edge ≈20–μm–thick region was observed after ultrasonic cleaning using dry ethanol.

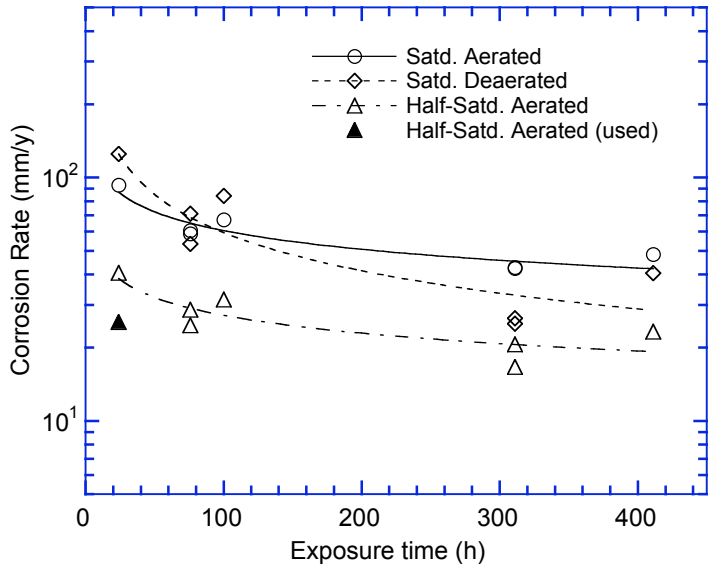

Figure 37.
Average corrosion rates for A533 Gr.–B in various boric acid solutions at 97.5°C

Figure 39 shows a schematic representation for the corrosion of low–alloy steel investigated in concentrated boric acid solution. Based on post–test examination of corrosion test specimens, we explain the most relevant evidences for the corrosion mechanism as follows:

(a) In the deaerated condition, the solution becomes pale blue but remains clear, i.e., Fe^{2+} ion dissolution. In the aerated condition, the solution becomes reddish and contains brownish-black deposit around the flask, i.e., Fe^{2+} or $Fe(OH)_3$, etc.,

(b) Gas bubbles generate and travel upward very vigorously around the A533 Gr.–B ring samples, i.e., hydrogen formation, under both aerated and deaerated conditions,

(c) Sample surface becomes dark indicating formation of a black scale, i.e., Fe_3C residue collects on the surface of the corroding samples, under both aerated and deaerated conditions.

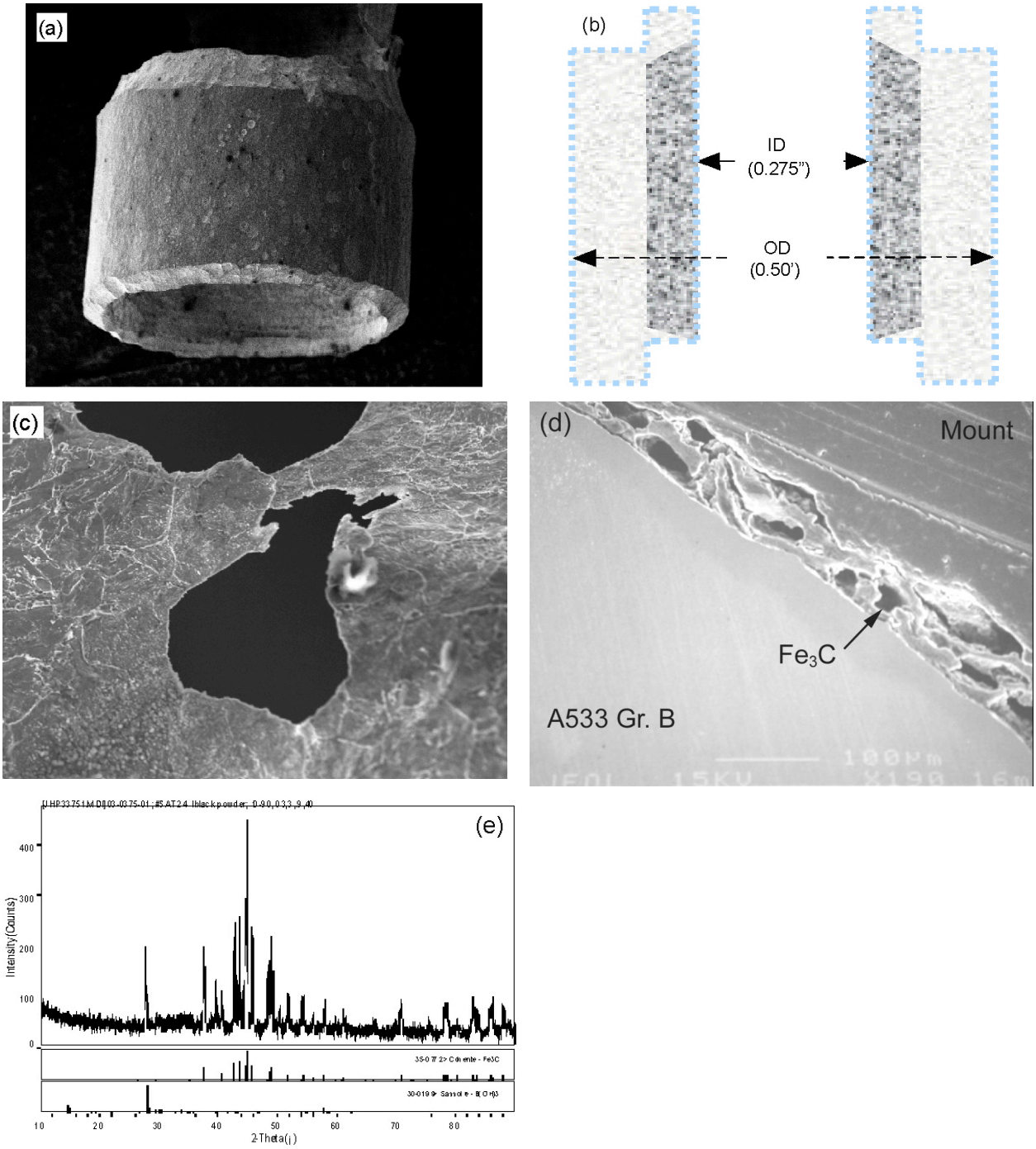

Figure 38. Geometry and metallographic evaluation of A533–Gr. B ring specimen exposed to deaerated saturated boric acid solution at 97.5°C for 411 h. (a) after ultrasonic cleaning, shape of A533–Gr. B specimen exposed for 411 h, (b) cross sectional view of the specimen as–fabricated (gray) and after the test (dark), (c) SEM micrograph of the surface of the corroded specimen in (a) at the tip of the corroding edge, (d) cross section SEM micrograph of the edge of the corroded A533–Gr. B specimen in (a) showing ≈20–mm–thick porous region with Fe_3C phase dominating the surface, and (e) x-ray diffraction analysis of the black powder identifying Fe_3C as the major phase.

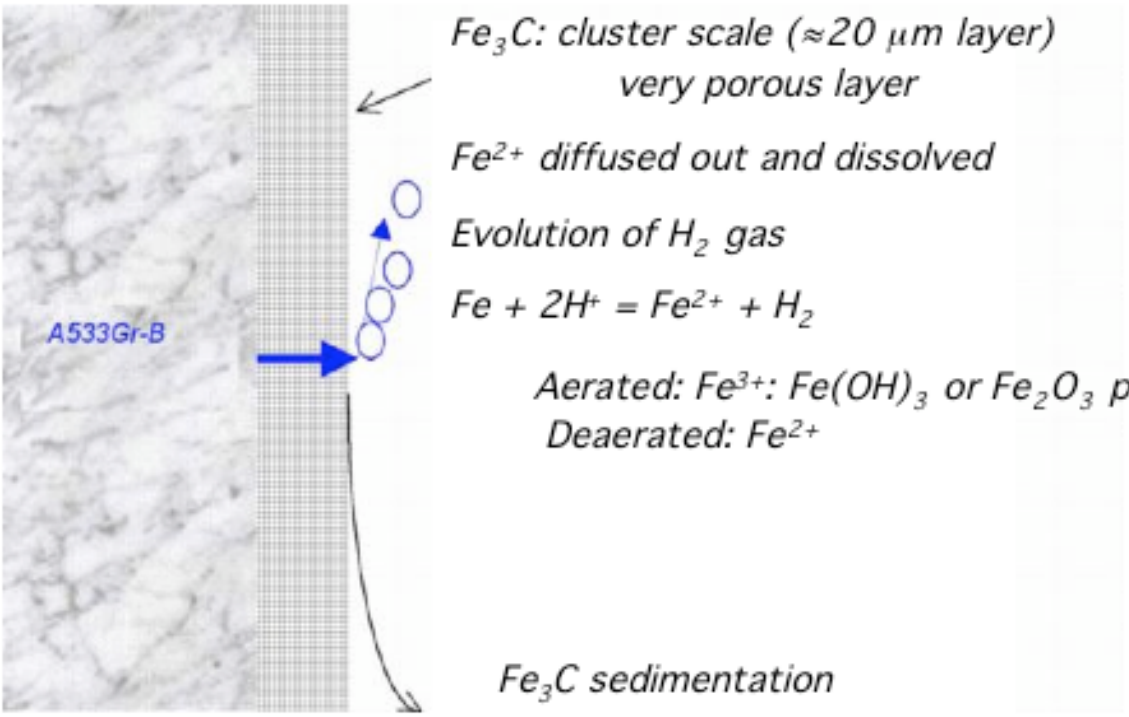

Figure 39. Schematic representation for the corrosion of low–alloy steel investigated in the concentrated boric acid solutions.

3.2.2 Molten H–B–O Environment at Ambient Pressure

Table 8 shows the corrosion data in dry H–B–O environments at 300, 260, and 150°C. The three H–B–O environments consist, respectively, of a (a) molten mixture of B_2O_3 + HBO_2 at 300°C, (b) molten HBO_2 at 260°C, and (c) a dry powder of HBO_2 + H_3BO_3 at 150°C. In the absence of moisture, no corrosion was observed for any of the materials. For corrosion to occur, the system requires a source of electron–capturing species such as protons (H^+).

Table 8. Corrosion test results in dry H–B–O environment at 300, 260, and 150°C.

Test Sample	Sample Weight (g)				Notes
	As Received	24-h test 300±9°C	26-h test 260±7°C	24-h test 154±4°C	
A533Gr-B (#9)	6.1925	6.1845	6.1832	6.1832	Little corrosion
A533Gr-B(#10)	6.2765	6.2722	6.2700	6.2700	detected
A600-2 (HT)	6.7356	6.7350	6.7342	6.7341	

Corrosion tests were also conducted in H–B–O system with additions of water. Boric acid was first heated to 260°C to obtain molten HBO_2, and water was added to the melt. The heat of evaporation cooled the system to a lower temperature, e.g., 150 and 170°C, respectively, for the two tests. The corrosion rates of A533 Gr.–B, Alloy 600, and 308 SS clad specimens in H–B–O environments at 150 and 170°C are given in Table 9.

Table 9. Test results in H–B–O system at different temperatures

Sample	As Received		150°C 45-h test		170°C 40-h test		Corrosion Rate (mm/y)	
	Wt. (g)	OD (in.)	Wt. (g)	OD (in.)	Wt. (g)	OD (in.)	150°C	170°C
A533 Gr.–B(#9)	6.1832	0.49900	3.5030	0.4530			127.94	
A533Gr.–B(#10)	6.2700	0.49900	3.9630	0.4470			144.63	
Alloy 600 CW-2	6.7341	0.49900	6.7346	0.4990			0.00	
A533 Gr.–B(#11)	6.1808	0.50000			4.9387	0.4870		36.157
A533 Gr.–B(#12)	6.1190	0.50000			5.8041	0.4942		16.132
Type 308 SS	6.7523	0.50000			6.7566	0.5000		0.00

The 308 SS and A533 Gr.–B specimens after an 40-h exposure in the H-B-O system at 170°C and ambient pressure are shown in Fig. 40a. An adherent film is seen on the 308 SS clad specimen and a non-adherent spalled scale is visible on the A533 Gr.–B specimen. Alloy 600 and A533 Gr.–B specimens tested in the H–B–O system at 150°C and ambient pressure for 45-h are shown in Figure 40b. Figure 41 shows the corrosion test results (closed diamonds) for A533 Gr.–B steel in H–B–O system with additions of water for test duration of 40–45 h. The results show significant corrosion of A533 Gr.–B steel in saturated solutions of boric acid at temperatures of 140–170°C, the corrosion rates range between ≈15–150 mm/y (0.6–6.0 in./y).

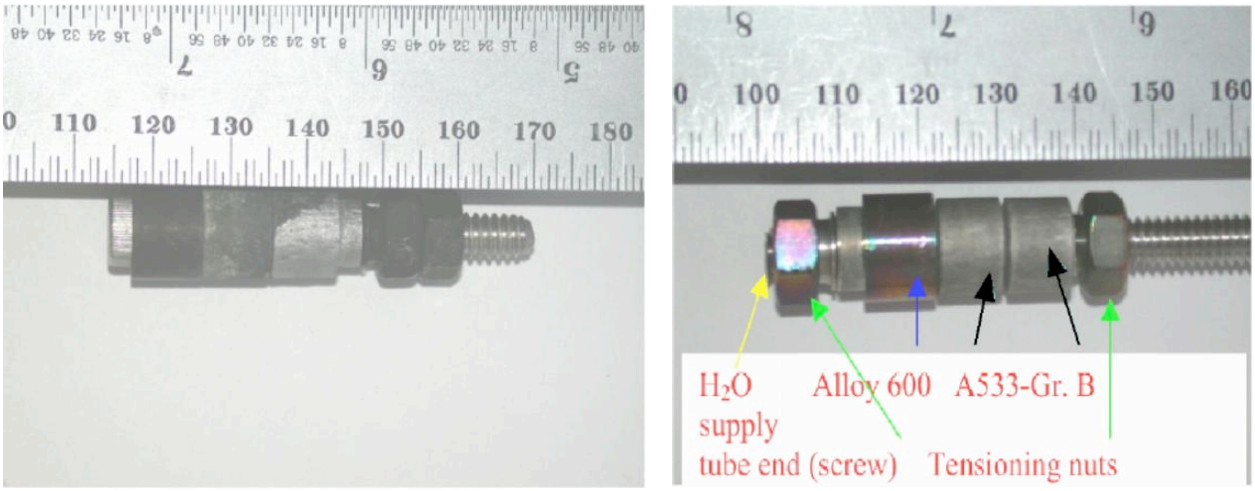

(a) (b)

Figure 40. Corrosion specimens tested in H-B-O system at 170°C and ambient pressure. (a) Type 308 SS and A533 Gr.–B specimens exposed for 40 h and (b) Alloy 600 and A533 Gr.–B specimens exposed for 45 h.

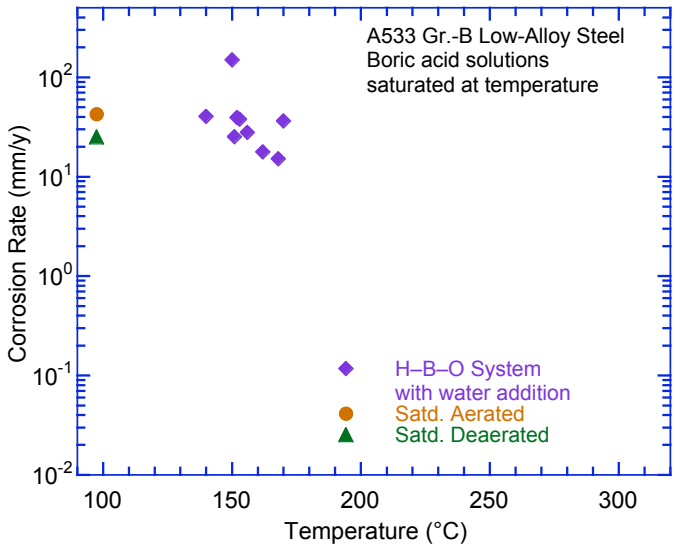

Figure 41.
Measured corrosion rates for A533 Gr.–B steel in H–B–O system with additions of water.

3.2.3 High–Temperature High–Pressure Boric Acid Solutions

Table 10 shows the observed weight changes and corrosion rates for A533 Gr.–B specimens tested at temperatures between 100 and 316°C in the room–temperature saturated boric acid (9090 wppm B). The results are plotted in Fig. 42. The results indicate that the corrosion rates for A533 Gr.–B steel are ≈4.5 mm/y at 100–150°C and decrease to ≈0.1 mm/y at 316°C. These test data show that corrosion rates of ≈5 mm/y are possible in room–temperature saturated boric acid solutions at temperatures 100–150°C and 12.4 MPa pressure. The rates fall to <1.0 mm/y at temperature ≥200°C. The implication of these results is that a wider window, from the standpoint of temperature and boric acid concentration, exits for the corrosion of low–alloy steel in a PWR system.

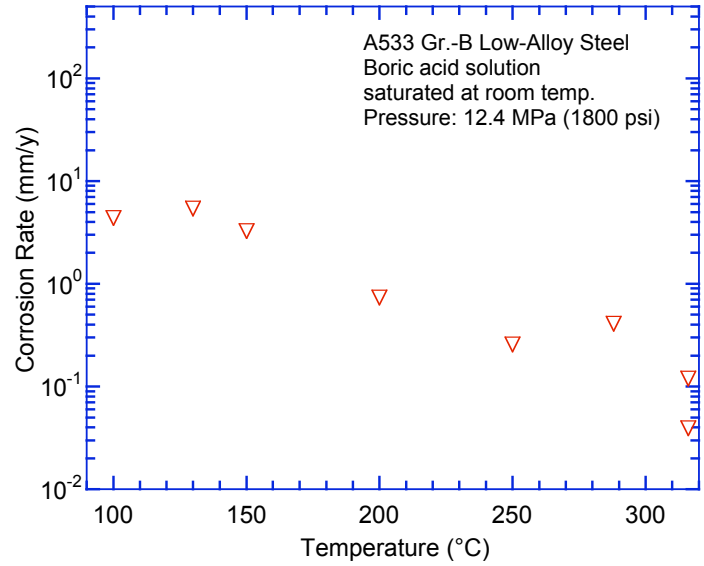

Figure 42.
Measured corrosion rates for A533 Gr.–B steel at high temperature and pressure in a room-temperature saturated boric acid solution (9090-wppm B) under hydrogen cover gas.

Table 10. Weight change data for A533-Gr. B tested at high temperature and pressure in a room-temperature-saturated boric acid solution (9090-wppm B) under hydrogen cover gas.

Temperature, Time	Sample Code	Wi (g)	Wf (g)	ΔW (g) = (Wi-Wf)	CR (mm/y)	Average CR (mm/y)
316°C, 24 h	LAS-1	0.27147	0.27128	0.00019	0.112	0.12
	LAS-2	0.26854	0.26834	0.00020	0.118	
	LAS-3	0.27466	0.27444	0.00022	0.129	
	LAS-4	0.27178	0.27158	0.00020	0.118	
316°C, 91 h	LAS-5	0.27667	0.27649	0.00018	0.0279	0.04
	LAS-6	0.27212	0.27181	0.00031	0.0481	
	LAS-7	0.26586	0.26554	0.00032	0.0497	
	LAS-8	0.27800	0.27780	0.00020	0.0310	
288°C, 24 h	LAS-9	0.27531	0.27485	0.00046	0.271	0.41
	LAS-10	0.30749	0.30668	0.00081	0.477	
	LAS-11	0.32178	0.32110	0.00068	0.400	
	LAS-12	0.24150	0.24068	0.00082	0.483	
250°C, 24 h	LAS-13	0.15433	0.15388	0.00045	0.265	0.26
	LAS-14	0.30678	0.30631	0.00047	0.277	
	LAS-15	0.27755	0.27702	0.00053	0.312	
	LAS-16	0.27583	0.27554	0.00029	0.171	
200°C, 24 h	LAS-17	0.28188	0.28105	0.00083	0.489	0.73
	LAS-18	0.28379	0.28236	0.00143	0.842	
	LAS-19	0.27710	0.27577	0.00133	0.783	
	LAS-20	0.26880	0.26741	0.00139	0.818	
150°C, 24 h	LAS-21	0.28680	0.28315	0.00365	2.148	3.25
	LAS-22	0.26527	0.25960	0.00567	3.337	
	LAS-23	0.31773	0.31307	0.00466	2.743	
	LAS-24	0.30575	0.29763	0.00812	4.779	
130°C, 24 h	LAS-25	0.25919	0.24959	0.00960	5.650	5.41
	LAS-26	0.29755	0.28793	0.00962	5.662	
	LAS-27	0.29414	0.28395	0.01019	5.997	
	LAS-28	0.30277	0.29538	0.00739	4.349	
100°C, 26 h	LAS-29	0.29876	0.29240	0.00587	3.455	4.37
	LAS-30	0.27977	0.27205	0.00713	4.194	
	LAS-31	0.32817	0.31972	0.00780	4.591	
	LAS-32	0.29065	0.28097	0.00894	5.259	

Capsule tests were also conducted on A533 Gr.–B, Alloy 600, and Type 308 SS samples to study corrosion under equilibrium conditions in the H-B-O system at high temperatures and pressures. Tests were conducted at temperatures between 170 and 316°C in a boric acid solution that was first saturated at room temperature. The temperature and pH_2O relationships for the boric acid system have been described in Section 2.2.

Weight changes for various specimens are listed in Table 11 and the visual appearance of some of the samples after testing is shown in Fig. 43. Samples exposed at 172°C showed a blossom–like deposit of hydrated iron-borate (Fig. 43a), whereas the samples exposed at higher temperatures showed only Fe_3O_4 deposits (Fig. 43b). For the A533 Gr.–B steel specimen exposed at 172°C, a very adherent layer of blossom-like deposits of iron borate was observed across the entire sample surface, resulting in a weight increase. However, even though iron oxide was deposited, all of the A533 Gr.–B disc samples lost weight. The weight changes are determined by cleaning the specimens to remove loose deposits and weighing the cleaned

Table 11. Weight and change in weight vs. temperature for the samples exposed to room-temperature saturated boric acid solution in the capsule tests for 68 h.

		A533 Gr.–B				Alloy 600			Type 308 SS		
Cell No.	Temp. (°C)	Initial Weight (g)	Final Weight (g)	Weight Change (g)	Corr. Rate (mm/y)	Initial Weight (g)	Final Weight (g)	Weight Change (g)	Initial Weight (g)	Final Weight (g)	Weight Change (g)
9	172	0.7240	0.7298	0.800[a]	–	0.3786	0.3786	0.0026	0.5690	0.5691	0.0053
10	235	0.7426	0.7421	-0.065	0.012	0.3376	0.3377	0.0180	0.5336	0.5337	0.0150
11	294	0.5950	0.5946	-0.072	0.011	0.5312	0.5312	0.0056	0.4609	0.4610	0.0087
12	316	0.5778	0.5776	-0.035	0.005	0.2905	0.2906	0.0034	0.4310	0.4311	0.0120

[a]An increase in weight because of the presence of very adherent iron borate blossom-like deposit across the entire sample surface.

specimens. The corrosion rates for A533 Gr.–B steel at 235–316°C are an order of magnitude lower than the rates observed in flowing room–temperature saturated boric acid solution (Fig. 42).

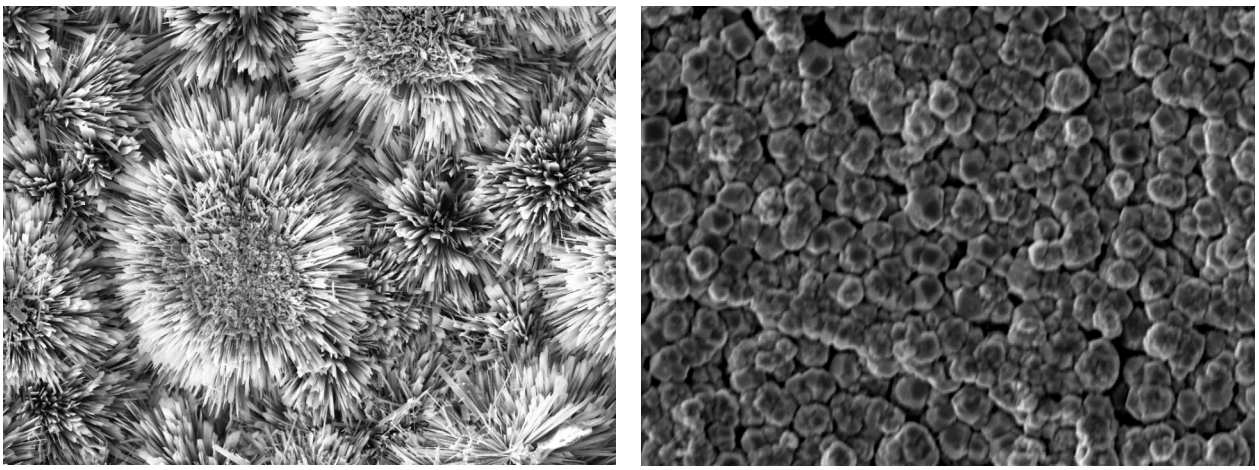

(a) (b)

Figure 43. (a) Blossom–like deposits of iron borate on A533 Gr.–B sample exposed at 172°C and (b) Fe_3O_4 deposits on the sample exposed at 294°C in room–temperature saturated boric acid solution inside a sealed capsule.

Figure 44 shows the measured corrosion rates for A533 Gr.–B steel in various boric acid solutions. As stated earlier, the corrosion process in boric acid solutions depends primarily on the physical-chemical behavior of the H-B-O system with temperature. However, the stability of $[B(OH)_4]^-$ appears to be lower at higher temperatures. This would explain the temperature dependence of the corrosion rate shown in Fig. 44 as well as the dependence on B concentration shown in Fig. 37. For a thermally activated process, corrosion rates are expected to increase with increasing temperature. For temperatures above 130°C, the temperature dependence of the corrosion rate for A533 Gr.–B steel in saturated boric acid solutions is determined by the $[H_3O]^+$ concentration; for lower temperatures, corrosion of A533 Gr.–B steel appears to be a thermally activated process. As shown earlier in Fig. 9, the pH of room-temperature saturated boric acid solution showed little temperature dependence between room temperature and 100°C, i.e., pH = 3.26; this trend continues to 150°C.

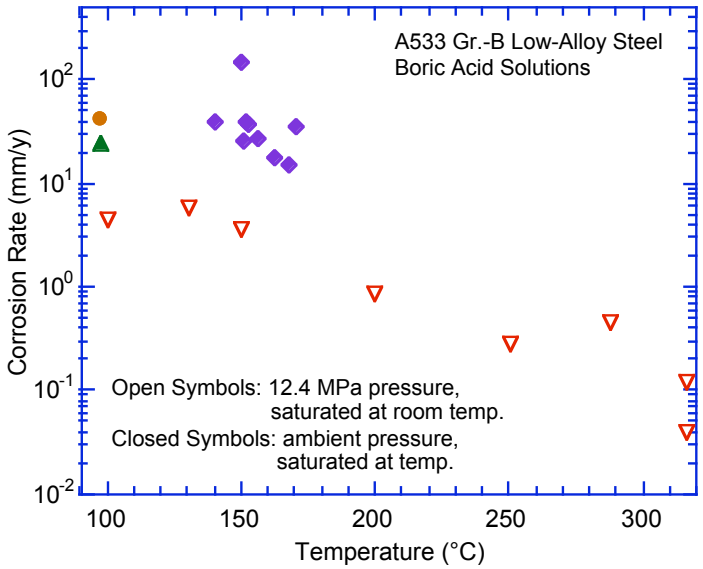

Figure 44.
Measured corrosion rates for A533 Gr.–B steel in various boric acid solutions.

Electrical conductance measurements of pure water and for aqueous boric acid solutions (containing 2,663 and 5,243 wppm B) were made over a temperature range of 25 to 350°C at the saturation vapor pressure.[11] Note that the B concentration in these solutions is below the room-temperature-saturated boric acid solution (9,090 wppm B), so all the $B(OH)_3$ would react with water to form $B(OH)_4^- + H_3O^+$ according to the reaction

$$B(OH)_3 + 2H_2O = B(OH)_4^- + H_3O^+. \quad (2)$$

The proton conductivity in solution is the highest among all the charged ions; the next highest ionic conduction species is $(OH)^-$ with a conductivity only ≈1/4 that of H_3O^+. Therefore, the electrical conductance data can provide relevant information on the proton activity in the system, and it is also useful for analysis of the data at higher temperatures i.e., T ≥100°C where a conventional pH probe could not be used. Results from this study showed a higher conductivity for the boric acid solutions than for the ultra-high-purity-water over the entire temperature range of 25 to 350°C (Fig. 45a), and increasing the boric acid concentration results in higher conductivity (Fig. 45b). All the conductivity values are higher at higher B concentrations over the entire temperature range investigated (25-350°C). However, as we see in Fig. 45c, from a plot of the slope (dσ/d[wppm B]) vs. T, we can identify three regimes of proton activity vs. boric acid concentration. At lower temperatures (T <75°C), i.e., Zone I in Fig. 45c, the conductivity increases with an increase in temperature. In Zone II (75 <T <150°C), the slope (dσ/d[wppm B]) vs. T is constant with temperature, but in Zone III (T ≥150°C), we see a negative dependence of proton conductivity on temperature.

The observed corrosion rate for the low–alloy steel seems to follow the conductivity variation with temperature. For a given boric acid or B concentration in aqueous solution, at T <100°C the corrosion rates for the low-Cr ferritic steels increase with temperature. At 100< T <150°C, the rates are fairly constant and at T >150°C, the rates decrease with an increase in temperature.

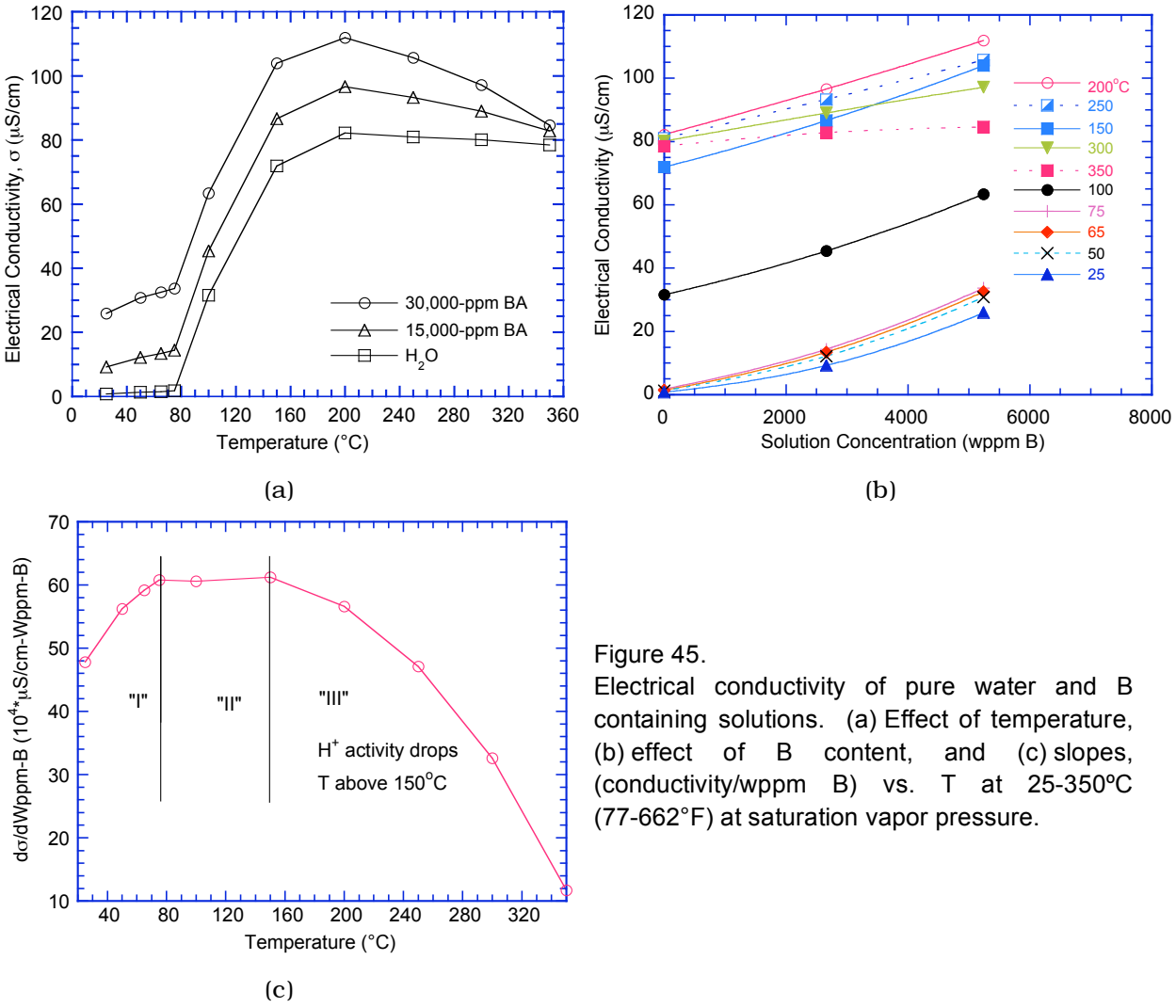

Figure 45.
Electrical conductivity of pure water and B containing solutions. (a) Effect of temperature, (b) effect of B content, and (c) slopes, (conductivity/wppm B) vs. T at 25-350ºC (77-662°F) at saturation vapor pressure.

3.2.4 Effect of Chromium Content on Corrosion Rate

It is fairly well known that the Cr content in an alloy can have a significant effect on the scale formation and corrosion performance of the alloy in aqueous environments. The effect of Cr content in the alloy on corrosion rate in aqueous environment that contains B and Li is of particular interest in PWRs, because Type 308 stainless steel weld overlay (with high Cr content) is being used on low–alloy steel reactor vessel head. To evaluate the role of Cr on the corrosion process, several alloys with varying Cr contents were exposed to room temperature saturated boric acid solution at 150, 288, and 316°C at a pressure of 12.4 MPa (1800 psig) under hydrogen cover gas. The room temperature saturated solution contained 9090 wppm B. Table 12 shows the nominal chemical compositions of the alloys used in the study. Table 13 lists the weight change data for various alloys exposed at 150, 288, and 316°C. In most cases, two specimens of each alloy were exposed.

Table. 12. Compositions of the alloys exposed in room-temperature-saturated boric acid solution.

Alloy	C	Cr	Mo	Ni	Si	Mn	Nb	V	Fe
H-1	0.096	1.0	0.47	0.08	0.09	0.001	0.002	-	Balance
H-2	0.096	2.1	0.48	0.06	0.09	0.001	0.002	-	Balance
H-3	0.094	4.5	0.46	0.06	0.13	0.005	0.005	0.002	Balance
H-6	0.098	9.5	0.50	0.07	0.01	0.002	0.005	0.001	Balance
H-9	0.094	11.9	0.49	0.05	0.01	0.001	0.010	-	Balance
308SS	0.029	21.1	0.39	9.37	0.56	1.27	-	-	Balance
Fe-25Cr	≈25 % Cr (Not analyzed in detail)								

Table 13. Weight change data for the alloys tested at high temperature and pressure in a room-temperature-saturated boric acid solution under hydrogen cover gas.

T°(C)	Wt.% Cr	Initial weight (g)	After 24-h exposure (g)	ΔW (g)	Corrosion rate (mm/y)	Average corrosion rate (mm/y)
150	0.2[1]					3.62
	1.0	0.06220	0.05720	5.0×10^{-3}	3.67	3.53
	1.0	0.05869	0.05408	4.6×10^{-3}	3.38	
	2.1	0.06312	0.05986	3.3×10^{-3}	2.39	2.14
	2.1	0.06323	0.06065	2.6×10^{-3}	1.89	
	4.5	0.06011	0.05799	2.1×10^{-3}	1.56	1.71
	4.5	0.05792	0.05539	2.5×10^{-3}	1.86	
	9.5	0.06306	0.06288	1.8×10^{-4}	0.13	0.12
	9.5	0.06305	0.06290	1.5×10^{-4}	0.10	
	11.9	0.01415	0.01411	4.0×10^{-5}	0.03	0.01
	11.9	0.01228	0.01231	-3.0×10^{-5}	-0.02	
	21.1[2]	0.46481	0.46482	-1.0×10^{-5}	-0.007	0
	21.1[2]	0.28696	0.28697	-1.0×10^{-5}	-0.007	
	25.0	0.18245	0.18243	2.0×10^{-5}	0.0147	0.02
	25.0	0.18742	0.18719	2.3×10^{-4}	0.17	
288	0.2[1]					0.45
	1.0	0.06010	0.05959	5.0×10^{-4}	0.374	0.41
	1.0	0.06357	0.06296	6.0×10^{-4}	0.448	
	2.1	0.06140	0.06084	5.6×10^{-4}	0.411	0.38
	2.1	0.06125	0.06078	4.7×10^{-4}	0.345	
	4.5	0.05798	0.05769	2.9×10^{-4}	0.213	0.20
	4.5	0.06117	0.06092	2.5×10^{-4}	0.183	
	9.5	0.06259	0.06245	1.4×10^{-4}	0.103	0.10
	9.5	0.06328	0.06315	1.3×10^{-4}	0.0954	
	11.9	0.01405	0.01399	6.0×10^{-5}	0.0440	0.07
	11.9	0.01298	0.01285	1.3×10^{-4}	0.0954	
	21.1[2]	0.44037	0.44031	6.0×10^{-5}	0.0279	0.03
	25.0	0.16327	0.16324	3.0×10^{-5}	0.0220	0.03
	25.0	0.19145	0.19140	5.0×10^{-5}	0.0367	
316	0.2[1]					0.12
	1.0	0.06433	0.06389	4.4×10^{-4}	0.323	0.30
	1.0	0.05832	0.05795	3.7×10^{-4}	0.271	
	2.1	0.06323	0.06294	2.9×10^{-4}	0.213	0.22
	2.1	0.06290	0.06260	3.0×10^{-4}	0.220	
	4.5	0.05926	0.05909	1.7×10^{-4}	0.125	0.13
	4.5	0.05734	0.05716	1.8×10^{-4}	0.132	
	9.5	0.06067	0.06058	9.0×10^{-5}	0.0660	0.06
	9.5	0.06160	0.06154	6.0×10^{-5}	0.0440	
	11.9	0.01347	0.01340	7.0×10^{-5}	0.0514	0.06
	11.9	0.01409	0.01400	9.0×10^{-5}	0.0660	
	21.1[2]	0.42574	0.42571	3.0×10^{-5}	0.0220	0.02
	25.0	0.18483	0.18483	0	0	0

[1]This row corresponds to A533 Gr.–B low alloy steel.
[2]This row corresponds to Type 308 weld metal.

Figure 46 shows a plot of average corrosion rate as a function of Cr concentration in the alloy. Also shown in the figure are the data developed on A533 Gr.–B steel (shown by open symbols) at the three temperatures. Several conclusions can be drawn from the data in Figure 46.

- The effect of increasing the Cr content of the alloy is to lower the corrosion rate at all temperatures of the study.
- At 150°C, there is a dramatic drop in corrosion rate when the Cr content of the alloy increased to 9 wt.%.
- The effect of an increase in temperature is to decrease the corrosion rate for the same boric acid concentration in the solution and for the same Cr content in the alloy.
- For a typical 308 SS weld metal with a nominal Cr content of 21 wt.%, the corrosion rate in room-temperature-saturated boric acid solution is in the range of 0.01-0.03 mm/y. The rate increases to 0.05–0.11 mm/y as the Cr content drops to 9 wt.%.

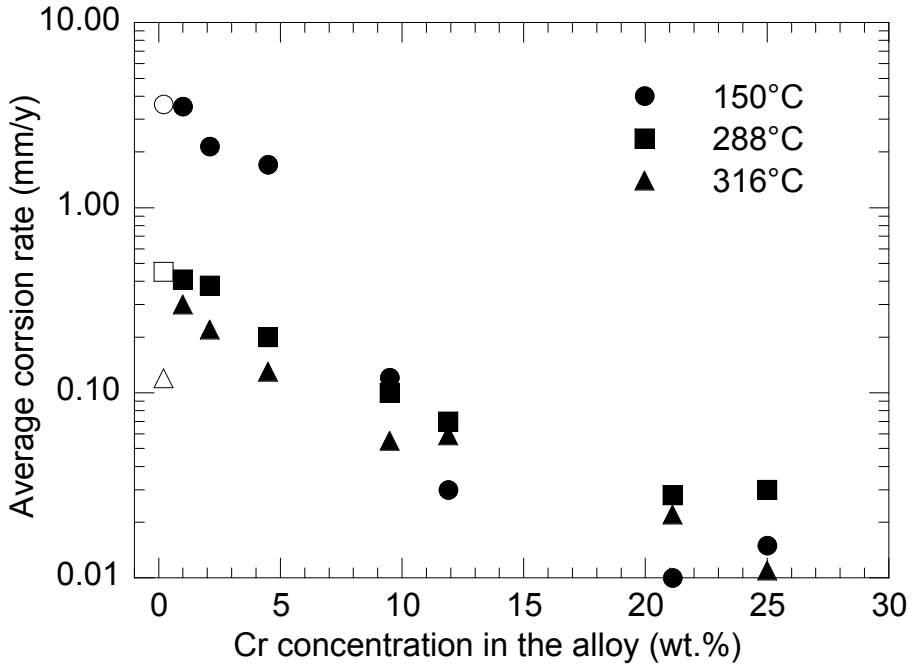

Figure 46. Effect of Cr concentration on the average corrosion rate in room-temperature-saturated boric acid solution at 150, 288, and 316°C and 12.4 MPa under H_2 cover gas.